Photoactive Self-cleaning Polymer Coatings by TiO_2 nanoparticle Pickering Miniemulsion Polymerization.

*Edurne González [a], Audrey Bonnefond [a], Mariano Barrado [b], Aurora M. Casado Barrasa [c], Jose M. Asua [a], Jose R. Leiza [a]**

a. POLYMAT, University of the Basque Country UPV/EHU, Kimika Aplikatua saila, Kimika Zientzien Fakultatea, Joxe Mari Korta zentroa, Tolosa Hiribidea 72, 20018 Donostia-San Sebastián, Spain. (jrleiza@ehu.es)

b. SGIKER, University of the Basque Country UPV/EHU, Joxe Mari Korta zentroa, Tolosa Hiribidea 72, 20018 Donostia-San Sebastián, Spain

c. Acciona Infrastructures Technology Centre, Spain

ABSTRACT

Titanium dioxide Pickering stabilized methyl methacrylate/n-butyl acrylate (MMA/BA) copolymer latexes were synthesized by miniemulsion polymerization. The particle size of the hybrid latexes was controlled by the concentration of TiO_2 used as stabilizer; the larger the concentration the smaller the particle size. The hybrid latexes formed coherent films with honey comb structures, the opacity of the films increased with the amount of TiO_2. The photocatalytic activity of the hybrid films was assessed by coating concrete specimens and analyzing the capabilities to degrade Rhodamine B under UV-light exposure. The films showed excellent self-cleaning activity and it was found that the photocatalytic activity index was little affected by the concentration of TiO_2 and the roughness of the film. The kinetic of the photocatalytic reaction was controlled by the diffusion of the Rhodamine B from the inner of the film to the interface.

KEYWORDS. Pickering stabilized latexes, TiO_2 nanoparticles, self-cleaning, photocatalytic activity, miniemulsion polymereization.

1 Introduction

Photocatalytic materials have gained extraordinary relevance in the last years due to their potential applications in fields such as photo-induced removal of pollutants from air and water, and self-cleaning and antibacterial materials [1-15]. Titanium dioxide (TiO_2) is the most widely investigated photocatalyst due to its high photoactivity, low cost, low toxicity and good chemical and thermal stability [16,17].

Currently, most photocatalytic coatings are prepared by the post-deposition of the catalyst onto a substrate, such as, glass, textiles, metals or polymers [2,5-9,12]. In the case of photocatalytic waterborne paints, the photocatalyst (TiO_2) usually is one of the components of the paint formulation that is blended with the waterborne dispersed polymer (binder) [3,10,11,15]. This often leads to the aggregation of the TiO_2 reducing its activity efficiency. A way to reduce the aggregation of the TiO_2 is by integrating it in the film forming waterborne polymer/inorganic hybrids [18-20]. However, the photocatalytic efficiency requires the presence of TiO_2 at the surface of the film; good distribution of TiO_2 in the polymer film does not guarantee high performance in photocatalysis. Thus, core-shell particles with the TiO_2 in the core and the polymer in the shell lead to a fine dispersion of the titania in the film, but to a poor catalytic efficiency because the TiO_2 is not accessible. Therefore, the morphology of the hybrid particles should be such that it allows an easy formation of a film with the surface covered by TiO_2. A way of achieving this goal is to place the TiO_2 at the surface of the hybrid polymer particle.

The morphology of the hybrid particles depends on the interplay between thermodynamics and kinetics, and hence it depends on the nature of the components of the polymerization recipe and the polymerization strategy used in the synthesis [21-24]. Among the different polymerization strategies aiming at producing hybrid latexes with the inorganic materials at the surface, polymerization of Pickering stabilized systems is advantageous [25]. In these systems the stability of the dispersion is provided by solid particles (often inorganic nanoparticles (NPs)) adsorbed on the oil/water interface. This allows avoiding (or at least substantially reducing) the use of conventional surfactants whose migration during film formation often causes poor gloss and adhesion, and high water sensitivity.

Strong adsorption of the inorganic particles at the oil-water interface is needed to ensure the formation of the desired particle morphology. A key parameter in the adsorption is the wettability of the NPs at the oil/water interface that can be estimated by the three-phase contact angle (θ_{Now}). Maximum adsorption energy is achieved for $\theta_{Now} = 90°$, namely for a particle that has half of its surface area in the aqueous phase and half in the oil phase [26-28]. The equilibrium shifts away from the interface as θ_{Now} separates from 90º. Because of geometrical reasons, water-in-oil dispersions are usually obtained when $\theta_{Now} > 90°$ whereas $\theta_{Now} < 90°$ yields oil-in-water dispersions [26]. Under equilibrium, the particles partition is between the aqueous phase and the interface for $\theta_{Now} < 90°$, and between the oil phase and the interface for $\theta_{Now} > 90°$. The high energy of adsorption in the vicinity of $\theta_{Now} = 90°$ is the reason for the higher stability of the Pickering stabilized emulsions as compared with those stabilized with conventional surfactants. As many inorganic materials are hydrophilic, surface modification is needed to increase the adsorption of the inorganic NPs at the interface, leading to highly stable oil-in-water dispersions [29-32].

In addition to avoiding the drawbacks associated to the use of conventional surfactants, it has been reported that Pickering stabilized latexes show improve mechanical properties in adhesives [33] and coatings [19,34-36]. These advantages have attracted the attention of the polymer community in the last years and a wide range of hybrid colloidal materials have been synthesized by means of emulsion [21,29,37-48] or miniemulsion polymerization [31,32,49-51].

The most commonly used Pickering stabilizers are clays [37,38,49,50] and silica NPs [21,29,31,32,39]. However other inorganic fillers, such as zinc oxide [40,41], magnetite [42], graphene [43,44] or cerium dioxide [51] have also been used. The use of titania NPs as Pickering stabilizers is scarce [30,45-48,52] and to the best of our knowledge none of these works have used titania NPs to stabilize film forming latexes for coating applications. Therefore, the photocatalytic efficiency of films cast form waterborne dispersions Pickering stabilized with TiO_2 remains to be demonstrated.

In this article, we report for the first time, the use of titania NPs as Pickering stabilizer of film forming latexes for coating applications and proof of the photocatalytic properties is provided. Polymerizations were carried out by means of surfactant-free Pickering miniemulsion polymerization using hydrophobically modified TiO_2 photocatalytic NPs. The effect of the amount of TiO_2 NPs on the morphology of the final latexes as well as on that of the film was studied. The photocatalytic efficiency of the hybrid polymer films was assessed performing self-cleaning test of the coatings applied in concrete specimens.

2. Material and methods

2.1. Materials

Methyl methacrylate (MMA) and n-butyl acrylate (BA) monomers were used as received from Quimidroga (Spain) . The modified TiO_2 NPs aqueous dispersion was provided by Fraunhofer

ISC (Germany) [53]. The TiO_2 was modified with acetyl acetone and para-benzene sulfonic acid. This modification renders the TiO_2 more hydrophobic than the pristine TiO_2. Octadecyl acrylate (Aldrich) was used as reactive costabilizer and 2,2′-Azobis(2-methylpropionitrile) (AIBN, Aldrich) as initiator. Doubly deionized (DDI, MiliQ quality) water was used throughout the work.

2.2. Synthesis of Pickering-Stabilized Latexes.

A copolymer of MMA and BA (50/50 wt %) commonly used for coating applications [54,55] was synthesized. Pickering stabilized latexes were sought because attempts to use physical blends of TiO_2 aqueous dispersions and acrylic latexes , yielded films where aggregation of the TiO_2 NPs could not be controlled, and besides, there was accumulation of the TiO_2 NPs at the substrate-film interface, which reduced substantially the performance of the nanocomposite films in the air-film interface.

Pickering-stabilized miniemulsions were prepared using the formulations given in Table 1. The challenges related with the industrial implementation of this process have been recently reviewed [56]. The oil phase was prepared by mixing the main monomers (MMA and BA; 50/50 wt %), the monomeric costabilizer (octadecyl acrylate) and the oil-soluble initiator (AIBN). This mixture was stirred magnetically for 5 min. The aqueous phase was obtained by diluting the original sulfonic acid modified aqueous TiO_2 NPs dispersion (original concentration ~12 wt % and particle size of 25 nm measured by Dynamic Light Scattering) in water and sonifying it for 10 minutes using a Branson 450 w (operating at 8-output control and 60% duty cycle) in order to achieve a good dispersion of the NPs in the aqueous phase. Both phases were mixed for 5 min under magnetic agitation and then sonified for 10 minutes using a Branson 450 w (operating at 8-

output control and 60% duty cycle). During sonication, the flask was immersed in an ice bath to avoid overheating.

After preparation, the miniemulsions were introduced into 0.1 L bottles and purged with nitrogen for 10 min. Then, the bottles were sealed and introduced into the thermostatic bath at 70 °C where they were tumbled end-over-end at 49 rpm for 15 h. Polymerizations with different TiO_2 NPs loadings were carried out.

Table 1 Formulation used for the synthesis of the Pickering stabilized latexes

	Component	wt %	Amount** (g)
Oil phase	MMA	4.8	3.84
	BA	4.8	3.84
	Octadecyl acrylate	0.4	0.32
	AIBN*	1	0.8
Water phase	TiO_2 NPs	5/10/20*	0.4/0.8/1.6
	Deionized water	90	72

*Respect to the main monomers (MMA/BA); ** For a recipe of 80 g latex

2.3. Latex and film characterization.

Conversion of the final latexes was measured gravimetrically. Dynamic Light Scattering (Zetasizer Nano ZS, Malvern Instruments) was used to measure the z-average diameter of the TiO_2 NP dispersion, miniemulsion droplets, and final polymer particles.

The stability of the miniemulsions was determined in a Turbiscan LAB (Formulaction) by placing the miniemulsion in a cylindrical glass cell which was completely scanned by a light source. The backscattered light, which depends on the droplet mean diameter and on the volume fraction, provided an easy measurement of the miniemulsion stability.

The contact angle at the TiO_2/monomer/water interface (ϑ_{Now}) was calculated as:

$$Cos\theta_{Now} = \frac{\gamma_w cos\theta_w - \gamma_o cos\theta_o}{\gamma_{ow}} \quad (1)$$

where γ_w and γ_o are the surface tensions of the aqueous phase and the monomer mixture, respectively, γ_{ow} the interfacial tension between the monomer mixture and the aqueous phase, and ϑ_w and ϑ_o are the contact angles of the TiO_2 NPs with the water phase and with the monomer mixture. These contact angles were measured by means of Washburn method [57] using a KSV30 tensiometer. The same equipment was used to determine the surface and interfacial tensions.

The morphology of both the final latex particles and the films was analyzed by Transition Electron Microscopy (TEM) and cryo-TEM in a TECNAI G2 20 TWIN (FEI) operating at an accelerating voltage of 200 kV in a bright field image mode. Polymer particles were observed without any staining. The preparation of samples for cryo-TEM involved first a vitrification procedure on a FEI Vitrobot Mark IV (Eindhoven, The Netherlands). One drop of the sample solution (~3 μL) was deposited in a copper grid (300 mesh Quantifolis, hydrophilized by glow-discharged treatment just prior to use) within the environmental chamber of the Vitrobot and the excess liquid was blotted away. The sample was shot into melting (liquid) ethane and transferred through a 655 Turbo Pumping Station (Gatan, France) to a 626 DH Single Tilt Cryo-Holder (Gatan, France) where it was maintained below -170 ºC (liquid nitrogen temperature).

The films cast at room temperature were trimmed at -40 °C using an ultramicrotome device (Leica EMFC6) equipped with a diamond knife. The ultrathin sections (100 nm) were placed on 300 mesh copper grids and were observed without further staining.

Atomic Force Microscopy (AFM) images of the film surface were obtained by a multimode Nanoscope IV (Veeco) working under taping mode with the TESP tips. X-ray photoelectron

spectroscopy (XPS) composition data and spectra were acquired on a SPECS (Berlin, Germany) instrument equipped with a Phoibos 150 1D-DLD analyzer and a monochromatic Al Kα X-ray source. Compositional survey and detail scans were acquired using a pass energy of 80 eV. High resolution spectra were acquired using a pass energy of 30 eV. The above data were taken at 90 º takeoff angle. Data analysis was performed with Casa XPS 2.3.16 Software to fit the signals to Gauss-Lorentzian curves, after removing the background (Shirley).

2.4. Self-cleaning properties.

Self-cleaning tests were performed in order to assess the photocatalytic activity of these coatings. The self-cleaning performance of a surface is usually measured by following the discoloration of an organic dye under UV radiation [58-61]. In this case, Rhodamine B based colorimetric tests were performed. Before the experiment, latexes were cast at room temperature over concrete substrates. Once the films were dried, they were dyed with a solution of Rhodamine B in ethanol. Rhodamine B dye exhibits a strong red color due to its highly delocalized Π- electrons , and discolorates by the action of radicals generated by the photocatalytic titania . Consequently, its discoloration can be followed by colorimetry.

The experimental set-up consisted of a test chamber where the specimens were placed horizontally and a light source located above their surface. The light intensity received by the specimens was $10 W/m^2$. The color of the samples was measured with a colorimeter. The results are expressed in the CIELAB system with L*, a* and b* colorimetric coordinates. As Rhodamine B applied onto materials gives an initial pink coloration, only the colorimetric coordinate a* was considered [62]. The measurements of a* were performed at different time intervals during 9 hours and two measurements were taken from each single sample.

The photocatalytic activity (Γ) was evaluated using the method proposed by Ruot et al. [62] based on the evolution of the a* parameter as follows:

$$\Gamma = C - Co \qquad (2)$$

where C is the dimensionless activity coefficient for the specimen that contains TiO_2 defined as:

$$C = \frac{A_t(a^*) - A(a^*)}{A_t(a^*)} \qquad (3)$$

and Co is the dimensionless activity coefficient for the blank sample (without TiO_2), where $A_t(a^*) = t \times a_0^*$ and $A(a^*) = \int_0^t a^*(t)dt$.

3. Results and discussion

The three phase contact angle value of the sulfonic acid modified TiO_2 NPs calculated by means of equation (1) was θ_{Now} =83° (γ_w= 46.6 mN/m, γ_o= 25.8mN/m. γ_{ow}= 15.8 mN/m, ϑ_w= 86 ° and ϑ_o= 87 °) which is close to the optimum value found by Gonzalez-Matheus et al. for silica NPs to obtain high solids content Pickering stabilized latexes [32].

Figure 1 displays the stability test (measured at 60 ° C) of the 10 % solids content miniemulsion prepared with 10 % weight based on monomers (wbm) of TiO_2. The miniemulsion presented excellent stability over a period of 3 hours. Very similar results were observed for the rest of the miniemulsions (with 5 and 20 wbm % of TiO_2).

Table 2 shows the droplet sizes of the prepared miniemulsions as well as the particle size and conversion of the final latexes. As it can be observed, the droplet size of the miniemusion decreased as the amount of hydrophobically modified TiO_2 was increased. This is a clear indication that the TiO_2 NPs were acting as efficient stabilizer, the larger the amount of TiO_2 used, the larger the area that could be stabilized and consequently, the smaller the droplet size.

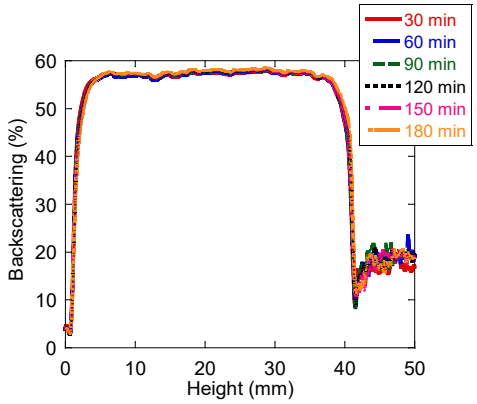

Fig. 1. Stability measurement of the miniemulsion prepared at 10 % s.c with 10 wbm % of sulfonic acid modified TiO_2. Measurement was performed at 60 ° C.

Table 2 Characteristics of the prepared Pickering stabilized miniemulsions and final latexes

TiO_2 (wbm %)	Droplet size (nm)	Particle size (nm)	Conversion (%)
5	307	1035	91
10	208	618	92
20	148	370	97

In all the reactions, the final average particle size was larger than the droplet size of the initial miniemulsion. Similar trends were observed by other authors when SiO_2 or CeO_2 NPs were used as stabilizers [32,51].

The increment in the particle size shows the occurrence of coalescence of monomer droplets (and/or polymer particles) during polymerization. Nevertheless, it is worth pointing out that no macroscopic coagulum was observed in any case after filtering the latexes through a mesh of 530 μm. The fact that the miniemulsion droplets were stable (see Figure 1), but the system destabilized upon polymerization strongly suggests that the reason for the droplets coalescence during the polymerization are changes occurring at the water-oil interface as polymer is formed. This modification in the nature of the interface, results in a variation of the interfacial tensions

and therefore, in a variation of the affinity of titania NPs to the oil/water interface affecting their adsorption energy.

Figures 2 and 3 show TEM and cryo-TEM micrographs of latexes stabilized with different amounts of TiO_2. All images showed a polydisperse distribution of mostly spherical particles. Moreover, TEM images show that the average particle size decreased with increasing amounts of TiO_2 while the surface coverage of the polymer particles (by titania NPs, as calculated from the particle sizes and final conversions displayed in Table 2) was similar for all the TiO_2 loadings. Furthermore, the shape of larger particles (Figure 2 (b) and (c)) tend to be less regular and exhibited a buckled surface. This could be an indication that these particles contained unreacted monomer at the end of the polymerization and their relatively stiff surface was deformed due to the decrease in volume caused by the evaporation of the monomer. In the cryo-TEM micrographs (Figure 3) taken for the Pickering latex stabilized with 10 wbm % of titania, the presence of the TiO_2 NPs at the polymer/water interface is clear. In the higher magnification images (Figure 3 (a) and (b)), a homogeneous surface coverage of the NPs in the polymer particles surface can be observed. Furthermore, the images show that little amount or no TiO_2 nanoparticles were present in the aqueous phase; namely most of the nanoparticles were adsorbed at the surface of the polymer particles.

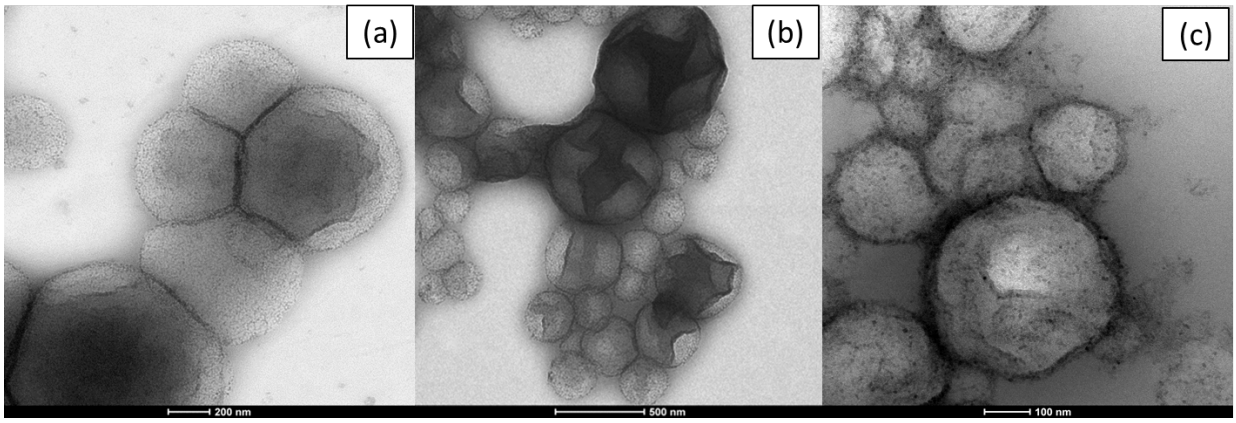

Fig. 2. TEM micrographs of latexes synthesized with different TiO_2 loadings: (a) 5 wbm %, (b) 10 wbm % and (c) 20 wbm %.

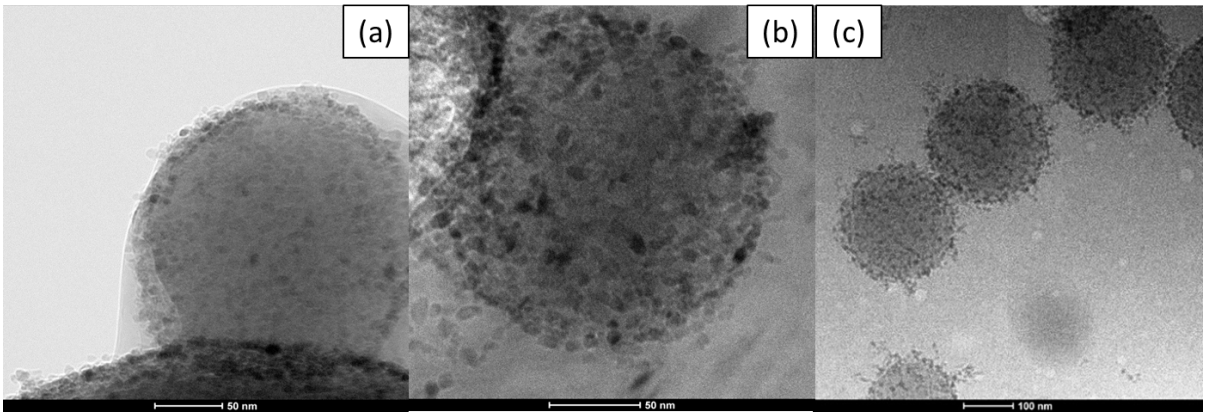

Fig. 3. Cryo-TEM micrographs of latex synthesized with a TiO_2 loading of 10 wbm %.

Figure 4 shows pictures of the films cast at room temperature. All the latexes were film-forming at room temperature following one of the requirements for application. White continuous films were obtained in all the cases and the opacity of the film increased as the amount of titania used as stabilizer was increased.

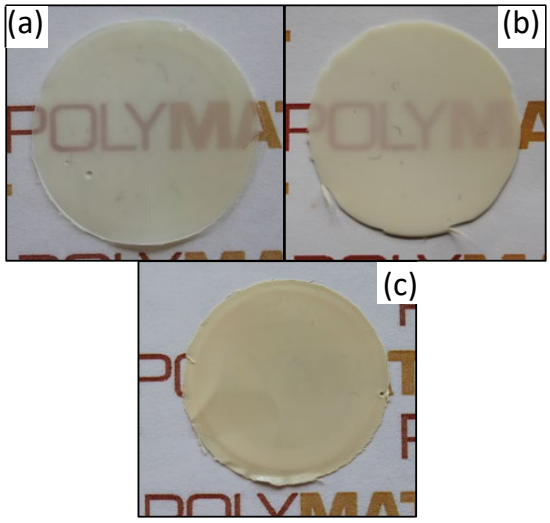

Fig. 4. Photographs of films casted at room temperature for Pickering latexes stabilized by different amount of TiO_2: (a) 5 wbm %, (b) 10 wbm % and (c) 20 wbm %.

Figure 5 presents TEM micrographs of the cross-section of these films. It is clearly observed that the TiO_2 NPs located at the surface of the polymer particles, create a continuous inorganic NPs network in the final film. It can also be observed that higher TiO_2 NPs loading led to larger aggregates of NPs at the interparticles interstices inside the film structure (see Figure 5). Note that it cannot be discarded that this accumulation of TiO_2 nanoparticles can be due to detachment of nanoparticles during the preparation of the film for the TEM analysis.

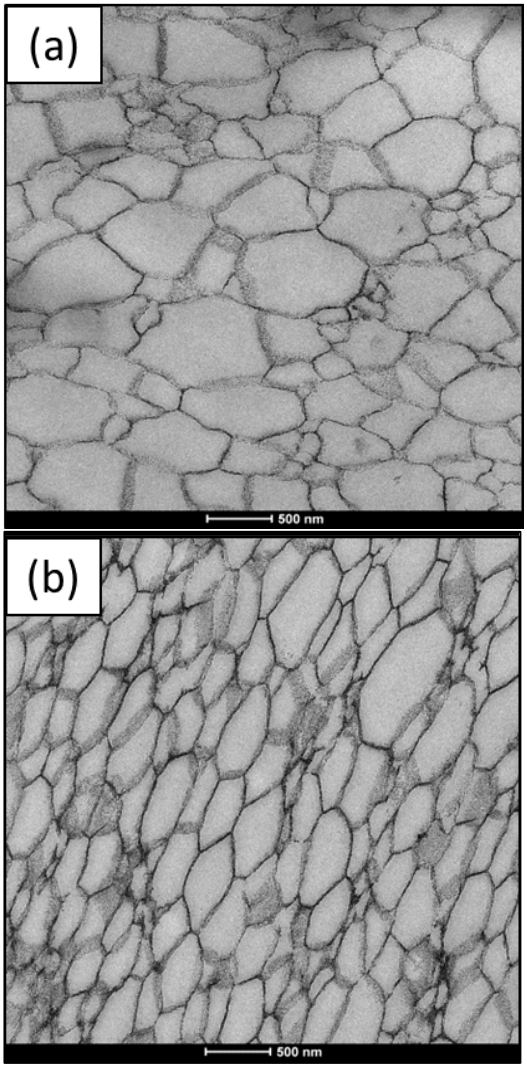

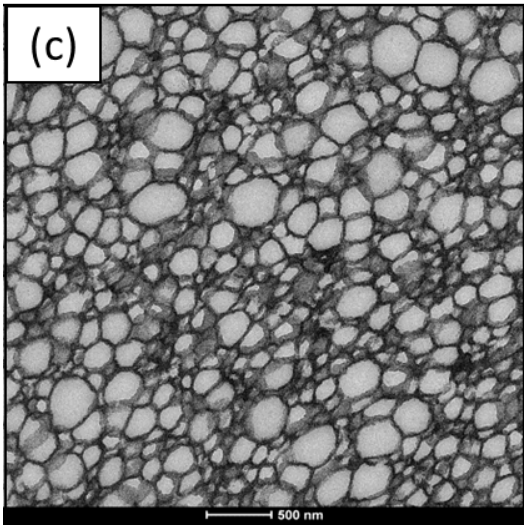

Fig. 5. TEM micrographs of the cross-sectioned films of the Pickering stabilized latexes by different amounts of TiO_2: (a) 5 wbm %, (b) 10 wbm % and (c) 20 wbm %.

The presence of inorganic NPs in the film was also analyzed by AFM at the air-film interface. Figure 6 presents the height and phase micrographs for films synthesized with 5, 10 and 20 wbm % of TiO_2. Table 3 displays the roughness (given as Ra, arithmetic average of the absolute values of the surface height deviations) calculated from the height images in a 10 μm x 10 μm region. The height images and the roughness data clearly indicated that the lower the amount of TiO_2 employed in the synthesis of the Pickering stabilized latexes, the higher is the film surface roughness. Furthermore, the phase images indicate that the surface is partially covered by the TiO_2 nanoparticles (see also Figure 7 for the higher magnification images) and that the coverage increases with the concentration of TiO_2. The increase of roughness as the amount of TiO_2 decreased can be attributed to the larger polymer particles sizes attained in the polymerization. In order to explain this, let us discuss film formation from Pickering stabilized latexes, which seems counterintuitive as the particles are covered by a shell of TiO_2 NPs. It has been demonstrated that the resistance to particle deformation produced by hard shell, is overcome by the capillary forces arising during water evaporation [63] (first step of film formation). The

capillary forces increase as the particle size decreases [64] and hence, better and smoother films are produced with latexes of smaller particles sizes. In addition, the differences in size of the polymer particles located at the top layer of the film (larger polymer particles were obtained when lower amounts of TiO_2 NPs were used) also affect roughness.

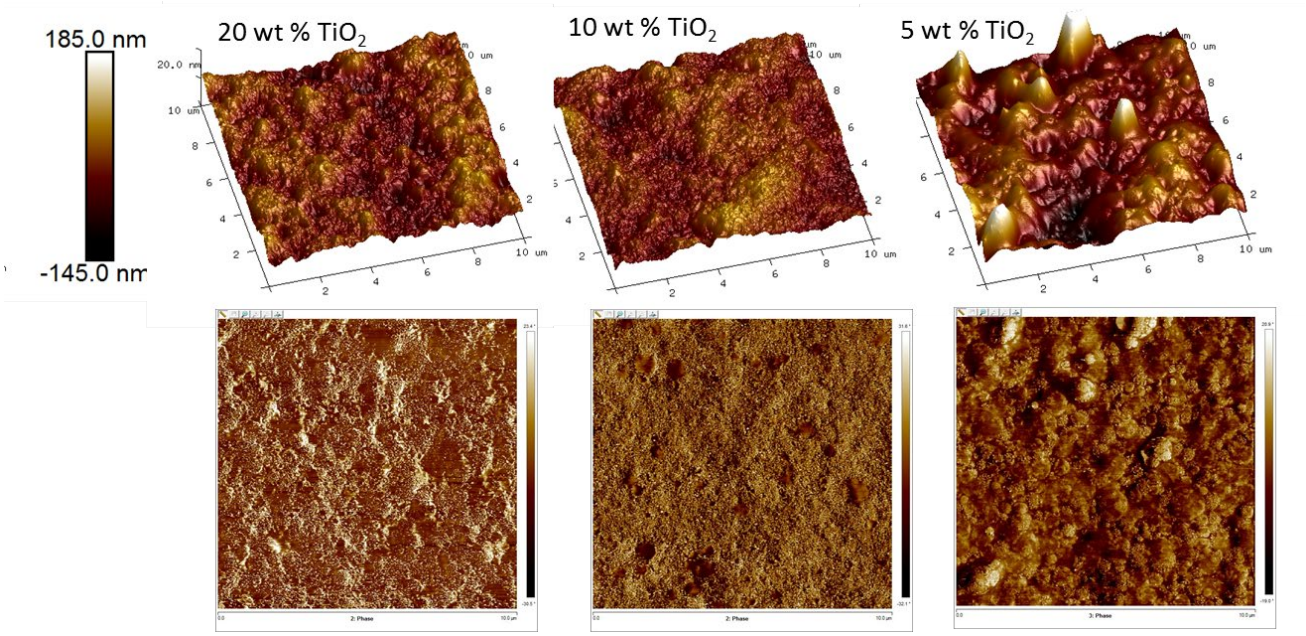

Fig. 6. AFM micrographs of the surface of the film of the latexes stabilized by 5, 10 and 20 wbm % of TiO_2. (Top) Height image and (bottom) phase image. Dimensions: 10 μm x 10 μm. It is demonstrated that the surface of the film is fully covered by titania. NPs.

Table 3 Roughness (Ra) of the air-film surfaces of the Pickering stabilized latexes calculated from the height AFM micrographs (10 x 10 μm region)

TiO_2 amount	20 wbm %	10 wbm %	5 wbm %
Ra (nm)	20	22	28

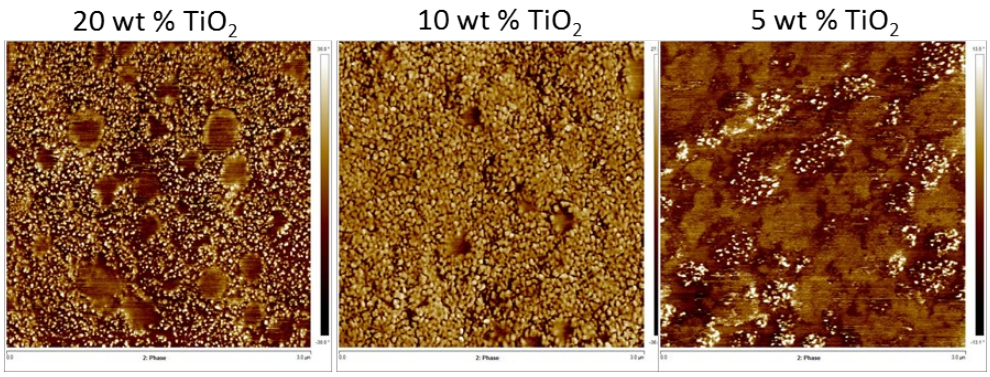

Fig. 7. AFM phase micrographs of the surface of the film of the latexes stabilized by 5, 10 and 20 wbm % of TiO_2. Dimensions: 3 µm x 3 µm.

The presence of the TiO_2 at the air-film interface and the roughness of the films are both very important features for photocatalytic applications, because the accessibility of the catalyst and the enhanced surface area favor the photocatalytic activity of the nanocomposite films (as the contaminants to be degraded must be adsorbed at the surface of the catalyst where the radicals are generated).

Therefore, in order to determine the concentration of Ti at the air-film interface of the films, XPS analyses were performed. The values of the concentration of Ti presented in Table 4 confirmed the qualitative data gathered by AFM; namely, the amount of Ti at the film surface increased with the concentration of TiO_2 employed during the synthesis.

In addition, XPS was also used to determine the distribution of the Ti along the film depth. For this purpose, depth profiling was carried out on both sides of the films for the film obtained with 10 wbm % of TiO_2. The air-film and substrate-film interfaces were bombarded for periods of 10 minutes up to 50 minutes using argon. The values at the air-film interface scattered between 3.2 8 (first layer) and 4.7 (after 50 min) At. % and at the substrate-film interface between 2 and 3.1 At. %, respectively.

Table 4 XPS measurement of Ti at air-film surfaces of the Pickering stabilized latex films

TiO_2 amount	20 wbm %	10 wbm %	5 wbm %
(Ti, atomic %)	5.5	3.2	0.5

Self-cleaning tests were performed in order to assess the photocatalytic activity of these coatings. It is noteworthy to mention that the photocatalytic activity of the TiO_2 NPs can potentially degrade the organic polymer too. Even if no polymer degradation was observed in the tested samples after the experiment, it should be mentioned that these tests were not long enough to conclude about this part.

Figure 8 shows pictures of the Rhodamine B dyed films cast over concrete substrates before and after being exposed to UV light. The blank sample corresponds to a conventional MMA/BA (50/50 wt %) latex stabilized by sodium lauryl sulfate [63] without any titania. As it can be observed, after 9 hours of UV radiation, the blank latex film continued being pink colored, whereas the films made of the hybrid latexes presented a significant discoloration. Thus, it is demonstrated that hybrid films are able to decompose Rhodamine B photocatalitically and therefore present self-cleaning properties.

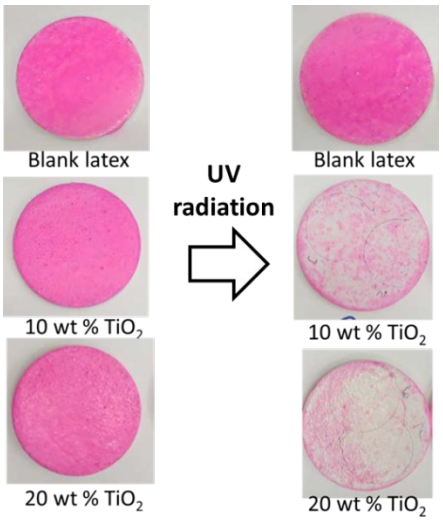

Fig. 8. Pictures of the Rhodamine B dyed films (cast over concrete substrates) before and after being exposed to UV light.

The photocatalytic activity index (Γ) was quantified from the time evolution of a* coordinate for each sample during the UV exposure. Figure 9 shows the evolution of both, a* coordinate and Γ. The coating without TiO_2 was not discolored at all during the exposure time; namely, a* coordinate did not vary (within the experimental error), indicating that there was no other physicochemical phenomena able to discolor Rhodamine B. For the hybrid coatings, the discoloration mainly occurred during the first 200 minutes, which is in good agreement with the observations of Ruot et al. [61] for two types of cement-based materials containing TiO_2 particles. A direct comparison of the photocatalytic activity, is better captured by the photocatalytic activity index (Γ, Figure 9 (b)) as the dependence of the initial a* coordinate value (different for each specimen) is circumvented. The three different coatings (with increasing amount of TiO_2) reached similar Γ values (0.73, 0.70 and 0.76, respectively) at the end of the test. However, the kinetics along the exposure time presented a trend that did not agree with the increased concentration of TiO_2 in the coated specimens; indeed, the specimen with 5 wbm % TiO_2 presented faster degradation of Rhodamine B than the specimen coated with the

nanocomposite with 20 wbm %. Nonetheless, the fastest discoloration was achieved by the coating with 10 wbm % of TiO_2. Others authors [66, 67] found also that the photocatalytic activity was independent of the loading of TiO_2 in the cementicious materials or that the size of the catalyst played a more important role. Ruot et al. [62], however, found that for cement paste Γ increased with loading of TiO_2, but for mortars the effect was not substantial. However, in these works the kinetics of the photocatalytic activity was hardly mentioned.

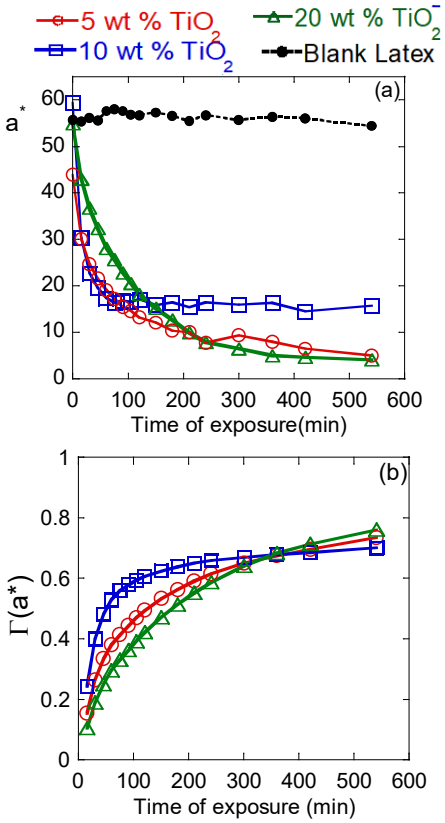

Fig. 9. Time evolution of the a* coordinate (a) and photocatalytic activity index (Γ, (b)) of latex films cast over concrete substrates.

Provided that the pollutant is available at the surface of the nanocomposite, the photocatalytic activity should be proportional to the concentration of TiO_2 and the available surface for adsorption of the organic compound to be degraded; i.e., Rhodamine B. AFM and XPS

demonstrated that the concentration of TiO_2 at the air-film interface increases with the amount of TiO_2 employed in the formulation, but interestingly the roughness measured by AFM shows the opposite trend; that is, the roughness increases by decreasing the amount of TiO_2 in the nanocomposites (although the difference is modest for the three concentrations). Figure 9 (b) shows that Γ is substantially higher for the nanocomposite film containing 10 wbm % TiO_2 than for those containing 5 and 20 wbm % during the first 150 min of UV exposure, which can hardly be explained by the surface concentration of TiO_2 and available surface area of the nanocomposite films; namely, the slightly higher roughness (surface area) of the nanocomposite containing 10 wbm % cannot justify the large difference in activity observed. Therefore, the only explanation that can be provided for this behavior is related with the availability of Rhodamine B at the film surface. The nanocomposite films absorb polar solvents (not shown) and hence when dying them with the Rhodamine B solution in ethanol (see experimental part), it can be speculated that Rhodamine penetrates to the interior of the nanocomposite film. Only Rhodamine B at the air-film interface participates in the photocatalytic reaction and hence there should be a diffusion of the Rhodamine B from the inner of the film to the interface where it is consumed. The rate of diffusion of Rhodamine B controls the discoloration reaction; the higher the concentration of TiO_2 in the film the lower the rate of diffusion. These competing mechanisms (photocatalytic reaction and Rhodamine B diffusion rates) can explain why the nanocomposite film with 10 wbm % of TiO_2 presents the fastest apparent photocatalytic reaction.

4. Conclusions

Miniemulsion polymerization using hydrophobically modified TiO_2 nanoparticles as the sole stabilizer were used to produce hybrid latexes made of MMA/BA that forms coherent films with

perfect honey-comb structures at room temperature. This one pot synthesis was used to prepare hybrid polymeric dispersions with different concentrations of TiO_2 that can be used as a photocatalyst to degrade pollutants and contaminants in paints, coatings and as additive in other formulations. In this work, the hybrid latexes were used to coat concrete specimens and test the self-cleaning capability of the films. It was shown that the coated films were able to degrade Rhodamine B. The photocatalytic activity index measured at the end of the UV exposure show no clear dependence of the concentration of TiO_2 employed during the synthesis; however the time evolution of the photocatalytic degradation was found to be controlled by the diffusion of the Rhodamine B from the inner of the film to the surface where the photocatalytic reaction occurred. The concentration of TiO_2 at the interface and the roughness of the film, seem to be less important than the diffusion rate of Rhodamine B regarding the photocatalytic activity of the hybrid coatings.

ACKNOWLEDGMENT

Financial support from the European Union (Limpid project FP7NMP-2012-2.2-6-310177), Ministerio de Economía y Competitividad (MEC, Ref. CTQ2014-59016-P), the Basque Government (GV IT-303-10) and Gipuzkoako Foru Aldundia (EXP 55/14) is gratefully acknowledged. The SGIKER UPV/EHU for the electron microscopy facilities of the Gipuzkoa unit is also acknowledged.

REFERENCES

[1] M.R. Dhananjeyan, E. Mielczarski, K.R. Thampi, P. Buffat, M. Bensimon, A. Kulik, J. Mielczarski, J. Kiwi, Photodynamics and surface characterization of TiO_2 and $Fe2O_3$ photocatalysts immobilized on modified polyethylene films, J. Phys. Chem. B 105 (2001) 12046-12055.

[2] C. Guillard, H. Lachheb, A. Houas, M. Ksibi, E. Elaloui, J.-M. Herrmann, Influence of chemical structure of dyes, of pH and of inorganic salts on their photocatalytic degradation by TiO_2 comparison of the efficiency of powder and supported TiO_2, J. Photochem. Photobiol. A 158 (2003) 27-36.

[3] N.S Allen, M. Edge, G. Sandoval, J. Verran, J. Stratton, J. Maltby, Photocatalytic coatings for environmental applications, Photochem. Photobiol. 81 (2005) 279-290.

[4] I.P. Parkin, R.G. Palgrave, Self-cleaning coatings, J. Mater. Chem. 15 (2005) 1689-1695.

[5] P. Raja, J. Bandara, P. Giordano, J. Kiwi, Innovative supported composite photocatalyst for the oxidation of phenolic waters in reactor processes, Ind. Eng. Chem. Res. 44 (2005) 8959-8967.

[6] T. Yuranova, R. Mosteo, J. Bandara, D. Laub, J. Kiwi, Self-cleaning cotton textiles surfaces modified by photoactive SiO_2/TiO_2 coating, J. Mol. Catal. A: Chem. 244 (2006) 160-167.

[7] G. Mascolo, R. Comparelli, M.L. Curri, G. Lovecchio, A. Lopez, A. Agostiano, Photocatalytic degradation of methyl red by TiO_2: comparison of the efficiency of immobilized nanoparticles versus conventional suspended catalyst, J. Hazard. Mater. 142 (2007) 130-137.

[8] L. Rizzo, J. Koch, V. Belgiorno, M.A. Anderson, Removal of methylene blue in a photocatalytic reactor using polymethylmethacrylate supported TiO_2 nanofilm, Desalination 211 (2007) 1-9.

[9] J. Medina-Valtierra, C. Frausto-Reyes, J. Ramírez-Ortiz, G. Camarillo-Martínez, Self-cleaning test of doped TiO_2-coated glass plates under solar exposure, Ind. Eng. Chem. Res. 48 (2008) 598-606.

[10] L. Caballero, K.A. Whitehead, N.S. Allen, J. Verran, Photoinactivation of Escherichia Coli on acrylic paint formulations using fluorescent light, Dyes Pigm. 86 (2010) 56-62.

[11] T. Martinez, A. Bertron, E. Ringot, G. Escadeillas, Degradation of NO using photocatalytic coatings applied to different substrates, Build. Environ. 46, (2011) 1808-1816.

[12] N. Miranda-García, S. Suárez, B. Sánchez, J.M. Coronado, S. Malato, M.I Maldonado, Photocatalytic degradation of emerging contaminants in municipal wastewater treatment plant effluents using immobilized TiO_2 in a solar pilot plant, Appl. Catal. B 103 (2011) 294-301.

[13] B. Jiang, X. C. Duan, Z. C. Zhou, Y. J. Cheng, G. C. Liu, Y. L. Liu, Synthesis and characterization of self-cleaning and anti-reflective SiO_2-TiO_2 nanometric films, Int. J. Inorg. Mater. 26 (2011) 375–380.

[14] C. Huang, H. Bai, Y. Huang, S. Liu, S. Yen, Y. Tseng, Synthesis of neutral SiO_2/TiO_2 hydrosol and its application as antireflective self-cleaning thin film, Int. J. photoenergy 2012 (2012) doi: 10.1155/2012/620764.

[15] M. Baudys, J. Krýsa, M. Zlámal, A. Mills, Weathering tests of photocatalytic facade paints containing ZnO and TiO_2, Chem. Eng. J. 261 (2015) 83–87.

[16] A. Fujishima, T.N. Rao, D.A. Tryk, Titanium dioxide photocatalysis, J. Photochem. Photobiol. C 1 (2000) 1-21.

[17] A. Fujishima, X. Zhang, Titanium dioxide photocatalysis: present situation and future approaches,

C. R. Chim. 9 (2006) 750-760.

[18] G. Diaconu, J.M. Asua, M. Paulis, J.R. Leiza, High-solids content waterborne polymer-clay nanocomposites, Macromol. Symp. 259 (2007) 305-317.

[19] N. Negrete-Herrera, J.-L. Putaux, L. David, F.D Haas, E. Bourgeat-Lami, Polymer/laponite composite latexes: particle morphology, film microstructure, and properties, Macromol. Rapid Commun. 28 (2007) 1567-1573.

[20] A. Bonnefond, M. Mičušík, M. Paulis, J. Leiza, R.A. Teixeira, S.F. Bon, Morphology and properties of waterborne adhesives made from hybrid polyacrylic/montmorillonite clay colloidal dispersions showing improved tack and shear resistance, Colloid Polym. Sci. 291 (2013) 167-180.

[21] N. Sheibat-Othman, E. Bourgeat-Lami, Use of silica particles for the formation of organic−inorganic particles by surfactant-free emulsion polymerization, Langmuir 25 (2009) 10121-10133.

[22] J.M Asua, Mapping the morphology of polymer–inorganic nanocomposites synthesized by miniemulsion polymerization, Macromol. Chem. Phys. 215 (2014) 458-464.

[23] M. Aguirre, M. Paulis, J.R. Leiza, T. Guraya, M. Iturrondobeitia, A. Okariz, J. Ibarretxe, High-solids-content hybrid acrylic/CeO_2 latexes with encapsulated morphology assessed by 3D-TEM, Macromol. Chem. Phys. 214 (2013, 214, 2157-2164.

[24] M. Mičušík, A. Bonnefond, Y. Reyes, A. Bogner, L. Chazeau, C. Plummer, M. Paulis, J.R Leiza, Morphology of polymer/clay latex particles synthesized by miniemulsion polymerization: modeling and experimental results, Macromol. React. Eng. 4 (2010) 432-444.

[25] A. Schrade, K. Landfester, U. Ziener, Pickering-type stabilized nanoparticles by heterophase polymerization, Chem. Soc. Rev. 42 (2013) 6823-6839.

[26] B.P. Binks, Particles as surfactants-similarities and differences, Curr. Opin. Colloid Interface Sci. 7 (2002) 21-41.

[27] R. Aveyard, B.P. Binks, J.H. Clint, Emulsions stabilized solely by colloidal particles, Adv. Colloid Interface Sci. 100–102 (2003) 503-546.

[28] S. Tcholakova, N.D. Denkov, A. Lips, Comparison of solid particles, globular proteins and surfactants as emulsifiers, Phys. Chem. Chem. Phys. 10 (2008) 1608-1627.

[29] A. Schmid, J. Tonnar, S.P. Armes, A new highly efficient route to polymer-silica colloidal nanocomposite particles, Adv. Mater. 20 (2008) 3331-3336.

[30] Y. Zhao, H. Wang, X. Song, Q. Du, Fabrication of two kinds of polymer microspheres stabilized by modified titania during pickering emulsion polymerization, Macromol. Chem. Phys. 211 (2010) 2517-2529.

[31] K. González-Matheus, G.P. Leal, C. Tollan, J.M Asua, High solids Pickering miniemulsion polymerization, Polymer 54 (2013) 6314-6320.

[32] K. González-Matheus, G.P. Leal, J.M. Asua, Pickering-stabilized latexes with high silica incorporation and improved salt stability, Part. Part. Syst. Charact. 31 (2014) 94-100.

[33] T. Wang, P.J. Colver, S.A.F. Bon, J.L. Keddie, Soft polymer and nano-clay supracolloidal particles in adhesives: synergistic effects on mechanical properties, Soft Matter 5 (2009) 3842-3849.

[34] S. Cauvin, P.J. Colver, S.A.F. Bon, Pickering stabilized miniemulsion polymerization: preparation of clay armored latexes, Macromolecules 38 (2005) 7887-7889.

[35] J.L. Amalvy, M.J. Percy, S.P. Armes, H. Wiese, Synthesis and characterization of novel film-forming vinyl polymer/silica colloidal nanocomposites, Langmuir 17 (2001) 4770-4778.

[36] A. Schmid, P. Scherl, S.P. Armes, C.A.P. Leite, F. Galembeck, Synthesis and characterization of film-forming colloidal nanocomposite particles prepared via surfactant-free aqueous emulsion copolymerization, Macromolecules 42 (2009) 3721-3728.

[37] N. Negrete-Herrera, J.-L. Putaux, L. David, E. Bourgeat-Lami, Polymer/laponite composite colloids through emulsion polymerization: influence of the clay modification level on particle morphology, Macromolecules 39 (2006) 9177-9184.

[38] R.F.A. Teixeira, H.S. McKenzie, A.A. Boyd, S.A.F. Bon, Pickering emulsion polymerization using laponite clay as stabilizer to prepare armored "soft" polymer latexes, Macromolecules 44 (2011) 7415-7422.

[39] P.J. Colver, C.A.L. Colard, S.A.F. Bon, Multilayered nanocomposite polymer colloids using emulsion polymerization stabilized by solid particles, J. Am. Chem. Soc. 130 (2008) 16850-16851.

[40] J.H. Chen, C.-Y. Cheng, W.-Y. Chiu, C.-F. Lee, N.-Y. Liang, Synthesis of ZnO/polystyrene composites particles by pickering emulsion polymerization, Eur. Polym. J. 44 (2008) 3271-3279.

[41] J. Jeng, T.-Y. Chen, C.-F. Lee, N.-Y. Liang, W.-Y. Chiu, Growth mechanism and pH-regulation characteristics of composite latex particles prepared from pickering emulsion polymerization of aniline/ZnO using different hydrophilicities of oil phases, Polymer 49 (2008) 3265-3271.

[42] Z. Xu, A. Xia, C. Wang, W. Yang, S. Fu, Synthesis of raspberry-like magnetic polystyrene microspheres, Mater. Chem. Phys. 103 (2007) 494-499.

[43] M.M. Gudarzi, F. Sharif, Self assembly of graphene oxide at the liquid–liquid interface: a new route to the fabrication of graphene based composites, Soft Matter 7 (2011) 3432-3440.

[44] J. Sun, H. Bi, Pickering emulsion fabrication and enhanced supercapacity of graphene oxide-covered polyaniline nanoparticles, Mater. Lett. 81 (2012) 48-51.

[45] T. Chen, P.J. Colver, S.A.F. Bon, Organic–inorganic hybrid hollow spheres prepared from TiO_2-stabilized pickering emulsion polymerization, Adv. Mater. 19 (2007) 2286-2289.

[46] X. Song, G. Yin, Y. Zhao, H. Wang, Q. Du, Effect of an anionic monomer on the pickering emulsion polymerization stabilized by titania hydrosol, J. Polym. Sci. A Polym. Chem. 47 (2009) 5728-5736.

[47] X. Song, Y. Zhao, H. Wang, Q. Du, Fabrication of polymer microspheres using titania as a photocatalyst and pickering stabilizer Langmuir 25 (2009) 4443-4449.

[48] G. Yin, Z. Zheng, H. Wang, Q. Du, Slightly surface-functionalized polystyrene microspheres prepared via pickering emulsion polymerization using for electrophoretic displays, J. Colloid Interface Sci. 361 (2011) 456-464.

[49] A. Bonnefond, M. Paulis, S.A.F. Bon, J.R. Leiza, Surfactant-free miniemulsion polymerization of n-BA/S stabilized by NaMMT: films with improved water resistance, Langmuir 29 (2013) 2397-2405.

[50] S.A.F- Bon, P.J. Colver, Pickering miniemulsion polymerization using laponite clay as a stabilizer, Langmuir 23 (2007) 8316-8322.

[51] N. Zgheib, J.-L. Putaux, A. Thill, F. D´Agosto, M. Lansalot, E. Bourgeat-Lami, Stabilization of miniemulsion droplets by cerium oxide nanoparticles: a step toward the elaboration of armored composite latexes Langmuir 28 (2012) 6163-6174.

[52] Y. Liu, X. Chen, R. Wang, J.H. Xin, Polymer microspheres stabilized by titania nanoparticles, Mater. Lett. 60 (2006) 3731-3734.

[53] P. Löbmann, M. Bockmeyer, B. Herbig, Stable suspensions of crystalline TiO_2 particles of hydrothermally treated sol gel precursor powders, US Patent 20090223412 A1, September 10, 2009.

[54] L.N. Butler, C.M. Fellows, R.G. Gilbert, Effect of surfactants used for binder synthesis on the properties of latex paints, Prog. Org. Coat. 53 (2005) 112-118.

[55] D. Urban, K. Takamura, Polymer dispersions and their industrial applications, Wiley-VCH Verlag GmbH, Weinheim, 2002.

[56] J.M. Asua, Challenges for industrialization of miniemulsion polymerization, Prog. Polym. Sci. (2014) 39, 1797-1826.

[57] E.W. Washburn, the dynamics of capillary flow, Phys. Rev. 17, (1921) 273-283.

[58] J. Chen, S.-C. Kou, C.-S. Poon, Photocatalytic cement-based materials: comparison of nitrogen oxides and toluene removal potentials and evaluation of self-cleaning performance, Build. Environ. 46 (2011) 1827-1833.

[59] N. Veronovski, A. Rudolf, M. Smole, T. Kreže, J. Geršak, Self-cleaning and handle properties of TiO_2-modified textiles, Fiber Polym. 10 (2009) 551-556.

[60] J. Chen, C.-S. Poon, photocatalytic construction and building materials: from fundamentals to applications, Build. Environ. 44 (2009) 1899-1906.

[61] N. Vero, S. Hribernik, P. Andreozzi, M. Sfiligoj-Smole, Homogeneous self-cleaning coatings on cellulose materials derived from TIP/TiO_2 P25, Fiber Polym. 10 (2009) 716-723.

[62] B. Ruot, A. Plassais, F. Olive, L. Guillot, L. Bonafous, L. TiO_2-containing cement pastes and mortars: measurements of the photocatalytic efficiency using a rhodamine B-rased colourimetric test, Sol. Energy 83 (2009) 1794-1801.

[63] E. Gonzalez, C. Tollan, A. Chuvilin, M.J. Barandiaran, M. Paulis, Determination of the coalescence temperature of latexes by environmental scanning electron microscopy, ACS Appl. Mater. Interfaces 4 (2012) 4276-4282.

[64] K. Gonzalez Matheus, G.P. Leal, J.M Asua, Film formation from Pickering stabilized waterborne polymer dispersions, Polymer (2015) DOI=101016/jpolymer 2015.05.053.

[65] M. Visschers, J. Laven, R. van de Linde, Forces operative during film formation from latex dispersions, Prog. Org. Coat. (1997), 31, 311-323.

[66] A. Strini, S. Cassese, L. Schiavi, Measurement of benzene, toluene, ethylbenzene and o-xylene gas phase photodegradation by titanium dioxide dispersed in cementitious materials using a mixed flow reactor, Appl. Catal. B 61 (2005) 90-97.

[67] G.Bolte, Photocatalysis in cement-bonded building materials, Cement International 3 (2005) 92-97.